Boiler tube corrosion characterization with a scanning thermal line

K. Elliott Cramer
National Aeronautics and Space Administration
Langley Research Center
4 Langley Blvd.
Mail Stop 231
Hampton, VA 23681

Ronald Jacobstein and Thomas Reilly
ThermTech Services, Inc.
2370 NE Ocean Blvd.
Stuart, FL 34996

ABSTRACT

Wall thinning due to corrosion in utility boiler waterwall tubing is a significant operational concern for boiler operators. Historically, conventional ultrasonics has been used for inspection of these tubes. Unfortunately, ultrasonic inspection is very manpower intense and slow. Therefore, thickness measurements are typically taken over a relatively small percentage of the total boiler wall and statistical analysis is used to determine the overall condition of the boiler tubing. Other inspection techniques, such as electromagnetic acoustic transducer (EMAT), have recently been evaluated, however they provide only a qualitative evaluation - identifying areas or spots where corrosion has significantly reduced the wall thickness.

NASA Langley Research Center, in cooperation with ThermTech Services, has developed a thermal NDE technique designed to quantitatively measure the wall thickness and thus determine the amount of material thinning present in steel boiler tubing. The technique involves the movement of a thermal line source across the outer surface of the tubing followed by an infrared imager at a fixed distance behind the line source. Quantitative images of the material loss due to corrosion are reconstructed from measurements of the induced surface temperature variations. This paper will present a discussion of the development of the thermal imaging system as well as the techniques used to reconstruct images of flaws. The application of the thermal line source coupled with the analysis technique represents a significant improvement in the inspection speed and accuracy for large structures such as boiler waterwalls.

A theoretical basis for the technique will be presented to establish the quantitative nature of the technique. Further, a dynamic calibration system will be presented for the technique that allows the extraction of thickness information from the temperature data. Additionally, the results of the application of this technology to actual waterwall tubing samples and *insitu* inspections will be presented.

Keywords: Infrared, Thermal, NDE, Corrosion, Boiler Tubes

1. INTRODUCTION

The inspection of large civil structures, such as utility water-wall tubing in boilers is a major challenge for power plant operators. Because of the size of these structures (typically 9,000 m^2 interior surface area) conventional NDE techniques such as ultrasonics, eddy currents and even conventional thermography, are limited in their usefulness. Ultrasonic and eddy current techniques typically use small area probes (approximately 6 cm^2 inspection area) which limit the total practical inspection area to only a small

percentage of the boiler water-wall. Additionally, the use of these techniques is very manpower intensive, imposing a practical limit on the total inspection area.

Recent developments have shown the advantages of infrared (IR) thermography for the detection of corrosion and disbonds in aircraft structures.[1,2,3] These techniques have typically involved heating with an IR source and the concurrent imaging of the induced temperature change with an IR camera. This offers a rapid method for detecting corrosion and quantifying its extent in single layer structures. In this application, the heating and imaging components of the system remain stationary during the measurement cycle. While conventional thermography can inspect large areas at a time (normally 1 m^2), disadvantages of this technique include the expense of the infrared camera and the large power requirement for the infrared heater. This latter disadvantage becomes especially significant when inspecting large, thick structures such as water-wall tubing.

This paper examines an alternate method for thermographically obtaining the thickness of the structure. It is patterned after a technique described by Maldague[4] where a sample moves at a constant velocity past a fixed linear heat source and is observed by an IR imager. Maldague demonstrates that the method is effective for the detection of disbonding in laminated samples.

Included are results from an alternate implementation of this system where the specimen is stationary and the line heat source and IR camera are translated together at a constant velocity. This implementation allows the rapid inspection of large structures such as power plant boilers. From the output of the IR camera, an image is reconstructed which yields the induced temperature changes at a fixed distance behind the line heat source.

This method has several distinct advantages over conventional NDE techniques. First, since the IR heater is held close to the object of interest, enabling a more efficient coupling of the energy into the specimen, the power requirements are reduced while preserving sensitivity. This method also enables very high inspection rates (in steel, speeds of 5 cm/s can be achieved). An additional advantage is that a linear array of detectors can replace the IR camera, significantly reducing the cost of the system.

Data will be presented from laboratory measurements on specimens with fabricated thinning to simulate material loss due to corrosion. A theoretical basis for relating the amount of thinning to the induced temperature change has been developed. The results of applying this technology to actual water-wall tubing samples and *in situ* boiler inspections will be shown.

2. EXPERIMENTAL TECHNIQUE

The current implementation of the scanned line source and imager is shown in Figure 1. The IR imager is a commercial radiometer with a cooled 256x256-element InSb (Indium - Antimonide) focal plane array detector. The radiometer's noise equivalent temperature difference (NEΔT), cited by the manufacturer, is 0.025°C when operating the detector in the 3 to 5 micrometer wavelength range. The radiometer produces images at both 30 frames per second output (video frame rate, in an RS170, format compatible with standard video equipment) and 60 frames per second output in a 12-bit, RS422 digital format. External optics, consisting of a wide-angle lens, using germanium optical elements, were used to increase the system field-of-view by a factor of approximately two. The expanded field-of-view of this lens is 22° in both the horizontal and vertical directions.

Focusing a commercially available 3000-watt quartz lamp, with an elliptical reflector behind the quartz tube, approximates a line of heat 40.6 cm in length and approximately 1.27 cm in width. The heat source and the IR imager are attached to a commercial linear scanning bridge. Quantitative time based analysis requires synchronization between the IR imager, the heat source and the scanning table. This synchronization is achieved by computer control of the application of heat, motion of the scanning table and data acquisition. The system can provide any scanning speed up to 30.5 cm/sec. For all cases presented in this paper, the maximum surface temperature change of the specimen above ambient was less than 10°C.

For low emissivity surfaces, it is necessary to enhance the emissivity by coating the surface. Paint is typically a good emissivity coating. If the specimen is painted, regardless of color, no additional surface coating is necessary. Unpainted metallic samples require the addition of an emissivity enhancing coating. For the results presented here, the metallic samples were treated with either water washable, nontoxic paint or flat black aerosol lacquer to increase the emissivity.

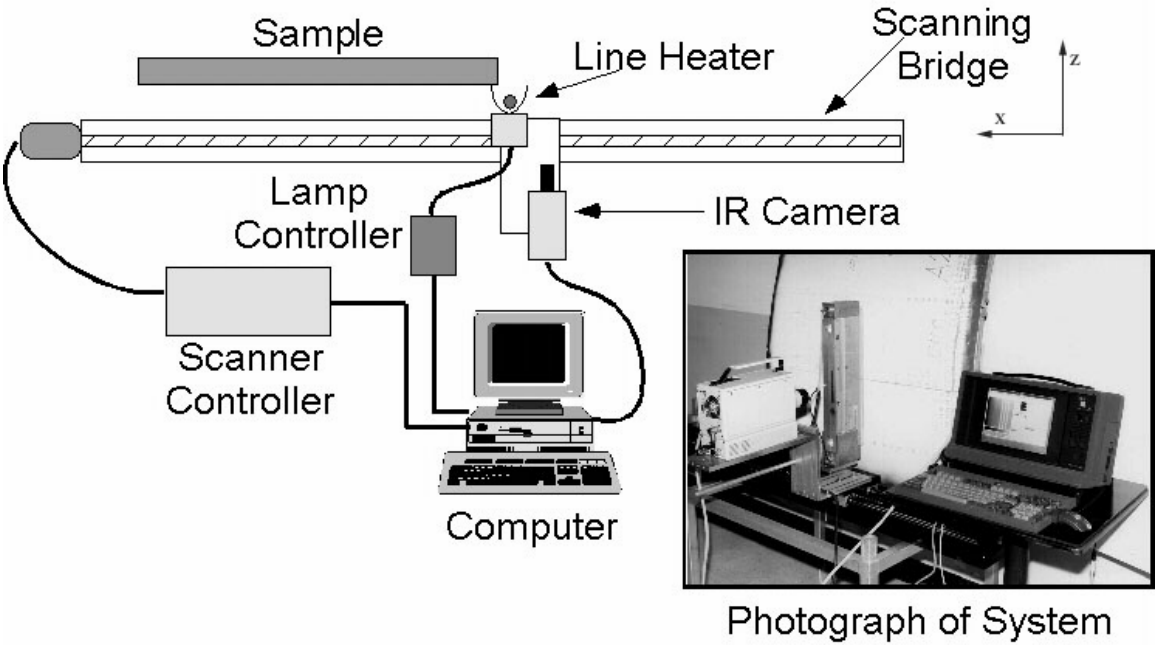

Figure 1 – Schematic and photograph of experimental setup used to implement moving line source technique.

The digital data from the radiometer were acquired and stored at rates up to 60 frames-per-second using a real-time image processing board in the control computer. The image processor board has 256 megabytes of image memory available for storage and is capable of real-time floating point processing of the incoming data. The imaging camera is moved with the heat source, enabling data acquisition at a fixed distance from the source. From a set of acquired images, a single image is then reconstructed that represents the induced temperature change at a fixed distance from the heat source. The reconstructed image is typically 256 pixels high and up to 1200 pixels wide (depending on the physical length of the sample, the speed of the scanner and the image acquisition rate). This reconstruction is currently done either in real-time by the image processor, or as post-processing analysis of the data. All of the data presented in the remainder of the paper (unless otherwise noted) were reconstructed in this manner.

3. STEADY STATE ANALYTICAL SOLUTION FOR MOVING LINEAR HEAT SOURCE

Assuming a medium of thickness L, with an infinitely long line source moving along the surface with a constant velocity v, and from a frame of reference moving with and centered on the heat source, it has been shown that the far field temperature distribution can be given by[5]:

$$T(x,z) = \frac{q}{Lv\rho c}\left[e^{-v\frac{(x+|x|)}{2\kappa}} + 2v \sum_{n=1}^{\infty} \mathrm{Cos}\left(\frac{n\pi z}{L}\right) \frac{e^{-\frac{vx+|x|\sqrt{(2n\pi\kappa/L)^2+v^2}}{2\kappa}}}{\sqrt{(2n\pi\kappa/L)^2+v^2}} \right], \quad (1)$$

where q is the input heat flux, ρ is the density, c the specific heat and κ the thermal diffusivity of the material.

Examination of Equation 1 indicates that when x is negative (behind the heat source) and the summation is approximately equal to zero, the temperature becomes a constant, q/(Lvρc). For lower velocities ($v < 2\kappa/L$), the condition necessary for the summation to be approximately zero is

$$x < \frac{2\kappa}{v - \sqrt{(2\pi\kappa/L)^2 + v^2}} \approx \frac{L}{\pi}. \quad (2)$$

At higher velocities ($v > 2\kappa/L$), the condition where the summation is zero is approximated when the distance behind the line source is equal to the thickness of the plate. When this occurs, the temperature in the far field behind the source is given by

$$T \approx \frac{q}{Lv\rho c}. \quad (3)$$

It can be seen from Equation 3 that the observed temperature of the surface is inversely proportional to the thickness of the material and can thus be used directly to measure the changes in thickness as long as the above condition is satisfied.

4. EXPERIMENTAL MEASUREMENTS OF SPATIAL RESOLUTION SPECIMENS

Figure 2 shows a diagram of a steel specimen fabricated to assess the validity of the relationship expressed in Equation 3. The specimen was 121.9 cm in length, 45.7 cm in width with a nominal thickness of 0.635 cm. A 10.2 cm wide region spanning the length of the specimen was reduced in thickness to 0.318 cm and three regions (25.4 cm in length and 5.1 cm in width separated by 12.7 cm) centered on the panel were reduced in thickness to 0.508 cm, 0.445 cm and 0.381 cm respectively.

Data were acquired on the specimen while moving the heat source and imager across the surface at a velocity of 3.81cm/s ($2\kappa/L$ for this case is approximately 1 cm/s). An image acquisition rate of 30 frames per second was used. Figure 3 shows an image and surface temperature profile obtained for a line of detectors 3.5 cm behind the line of heat. The relationship between the scanning speed and the separation distance between the line of heat and the detectors has been addressed in previous work[5]. It is difficult to perform an exact reduction of thermal data to thickness using Equation 3 since in practice q is unknown and ρ and c are only approximately characterized. Therefore a 0.635 cm thick region across the top of the specimen and a 0.318 cm thick region at the bottom were used to fit Equation 3 to the data in the center of the panel and provide an estimate of specimen thickness. The results of this data reduction, averaged over the area of the three interior material loss regions, and compared to the actual panel thickness are shown in Figure 4. It can be seen that while there is good agreement in some areas, in other areas the calculated thickness deviates from the actual by as much as 4.8%. This variation may be due to warping of the specimen that occurred during fabrication. This warping made it difficult to keep the line heat source parallel to the specimen during the entire length of the data collection scan.

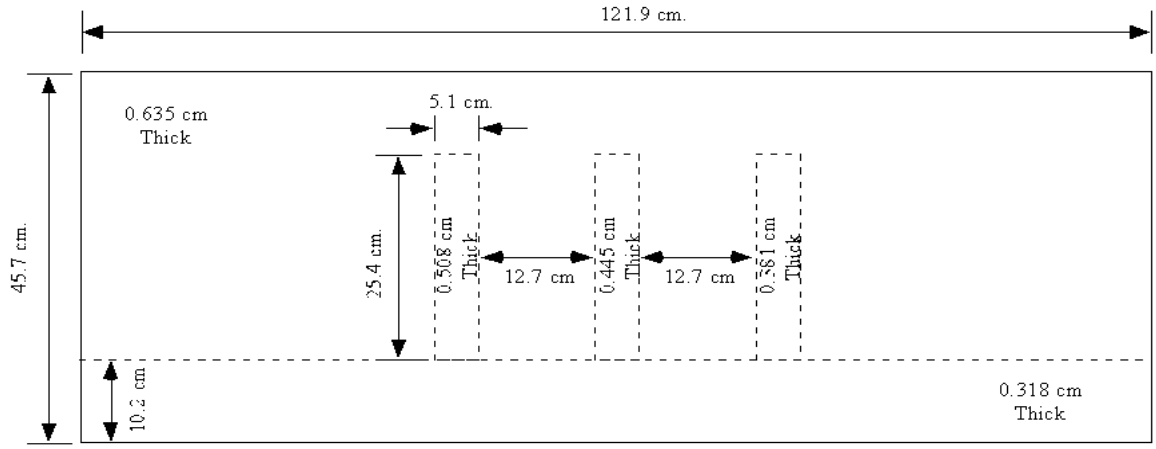

Figure 2 – Steel specimen, 0.635 cm thick, with three sets of material loss regions, 0.508 cm, 0.455 cm and 0.381 cm deep respectively, centered on the panel and separated by 12.7 cm. Each region is 5.1 cm wide and 25.4 cm long. A region 10.2 cm wide and spanning the length of the specimen was reduced in thickness to 0.318 cm.

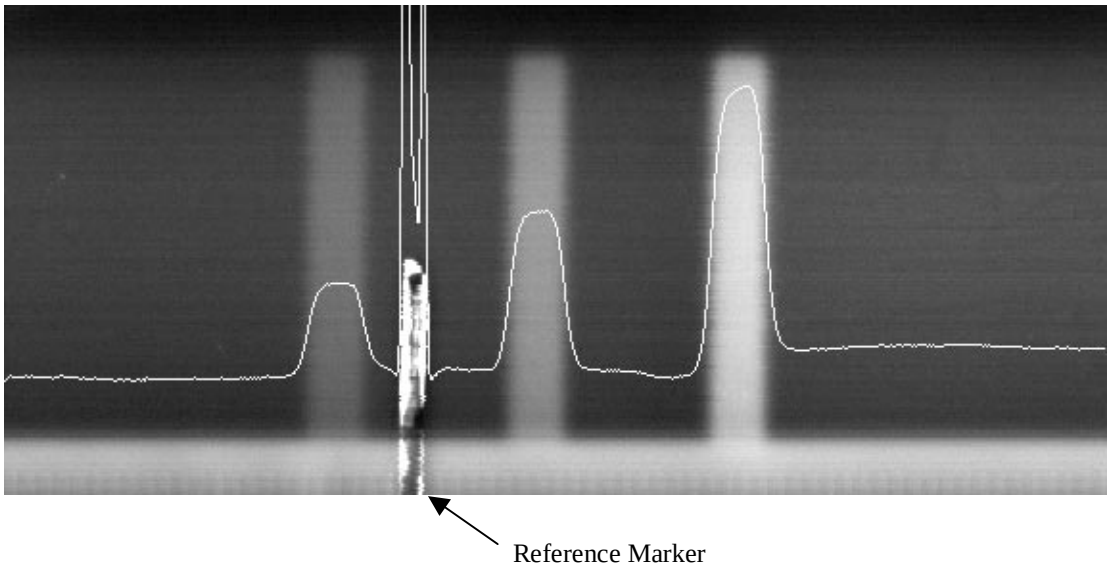

Figure 3 – Thermal line scanner image and surface temperature profile for steel thickness specimen. A reflective tape reference mark was placed on the surface of the specimen before imaging.

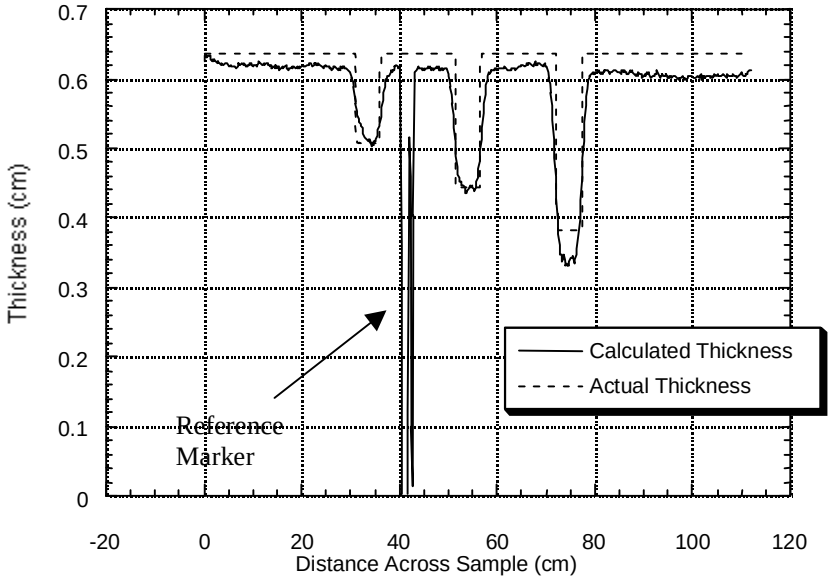

Figure 4 – Comparison of the actual thickness of the steel specimen with the thickness calculated from the thermal line scanner temperature data.

5. BOILER WATER-WALL TUBE DATA

To investigate the application of this technique to water-wall tubing, a large specimen (specimen #1) was removed from a commercial power plant and sectioned into manageable sized sub-sections. The specimen was 116.8cm in length and 26.7cm in width with tubes of outside diameter 3.2 cm and a nominal wall thickness of 0.7cm. A series of defects were artificially introduced into the sample by removing the entire wall thickness on one side of the sample to provide access ports for machining. Next, material loss regions were machined into the exposed inside walls of the tubing. Different sizes and depths of defects were introduced into the sample to provide a representative selection of material losses that may be found in operational boilers. Figure 5 provides a schematic of this laboratory sample, which shows the pattern of defects introduced. The defects were produced in the crown region of the tubes (± 20º of top-dead-center) only. Since the majority of the material loss in water-wall tubing occurs near the crown, this is a good approximation of the type of defects found on in-service boilers[6]. The surface of this specimen was sand blasted to remove any slag, and then was painted black using flat black aerosol lacquer to enhance the emissivity.

The results of scanning the water-wall tube sample are shown in the image in Figure 6. The sample was scanned at a speed of 6.3 cm/s and the separation distance (between line of heat and image reconstruction point) was 3.5 cm. All the machined defects can be detected in the resulting image. Since material loss does not typically occur in the webbing between the tubes (dark bands in Figure 6) these regions are ignored. Further it is possible to calibrate the results of the thermal imaging to measure tube thickness at points along the crown of the tube. Mechanical thickness measurements were made at various locations along tube number one (see Figure 5). These measurements were used to calculate a calibration constant ($v\rho c/q$) for Equation 3. A linear regression of the data was performed using the constant calculated from tube 1 to obtain thickness maps of the other three tubes. Figure 7 shows a plot of the thickness of two of the tubes (both thermal measurements and mechanical measurements) versus position measured from the left side of the sample as imaged. A region of the thermal image equal to ±20 degrees of the tube crown was averaged to produce the thickness plots.

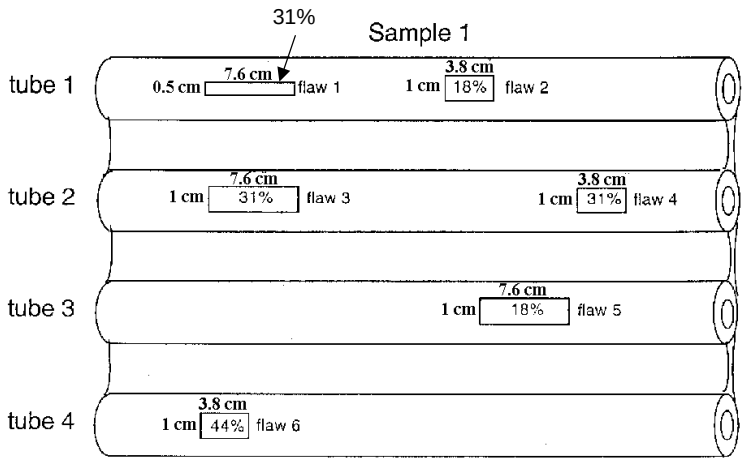

Figure 5 – Boiler water-wall tube specimen #1 with machined defect pattern.

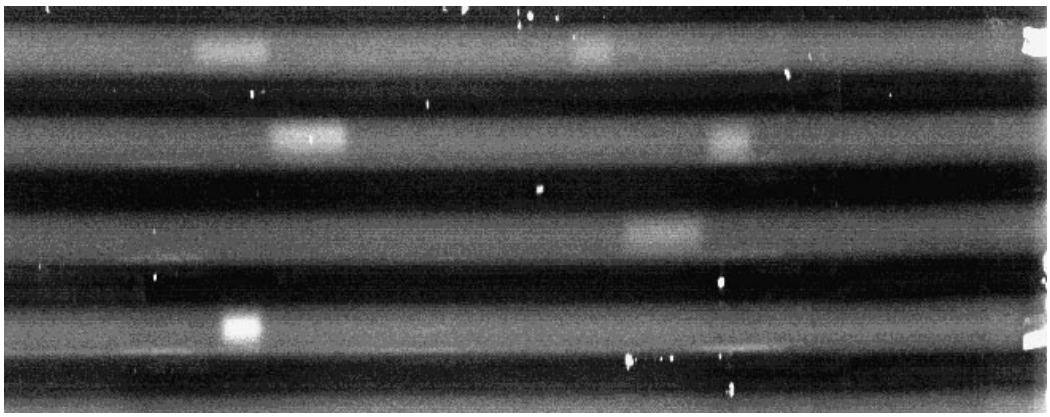

Figure 6 – Reconstructed thermal line scanner image showing machined defects in boiler water-wall tubing specimen #1.

To more closely simulate the conditions in an operational power plant, a second specimen (specimen #2) of the same size was also machined with a different series of material loss regions. The surface of this specimen was not sand blasted, but was subjected only to a high-pressure water wash. Then, water soluble black paint was applied. Two calibration standards of different thicknesses (0.38 cm and 0.63 cm respectively) were placed in the webbing region of the sample during inspection.

The results of scanning this specimen are shown in Figure 8. The sample was scanned at a speed of 2.54 cm/s with a separation distance of 3.5cm behind the line of heat. While the defects are still clearly visible, the reduced surface preparation results in noisier data. Since most of the additional noise occurs in the web region it can be ignored. The standards were then used to calculate the calibration constant for Equation 3, which was then used to calculate the specimen thickness at all points along the tube crowns. Thickness measurements (both calculated and from mechanical measurements) versus position are shown in Figure 9.

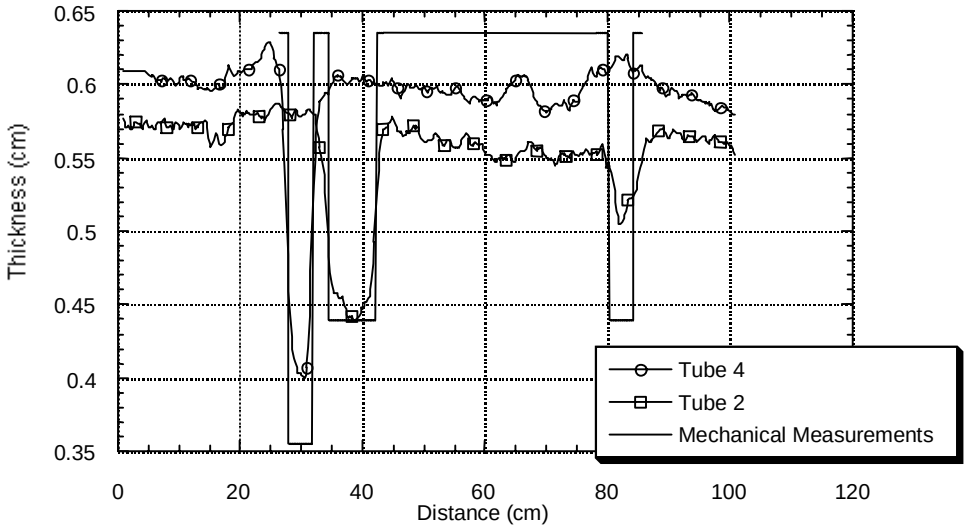

Figure 7 – Comparison of thickness measurements made both thermally and mechanically on boiler water-wall tubing specimen #1.

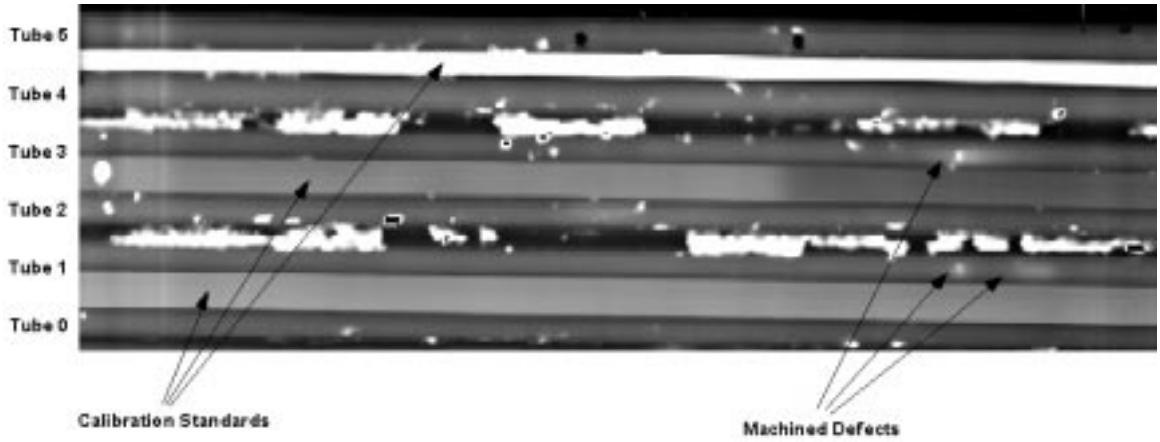

Figure 8 – Reconstructed line scanner image showing machined defects in boiler water-wall tubing specimen #2 with minimal surface preparation to simulate actual boiler conditions. Three calibration standards can be seen in the image, only the outermost two were used for image calibration.

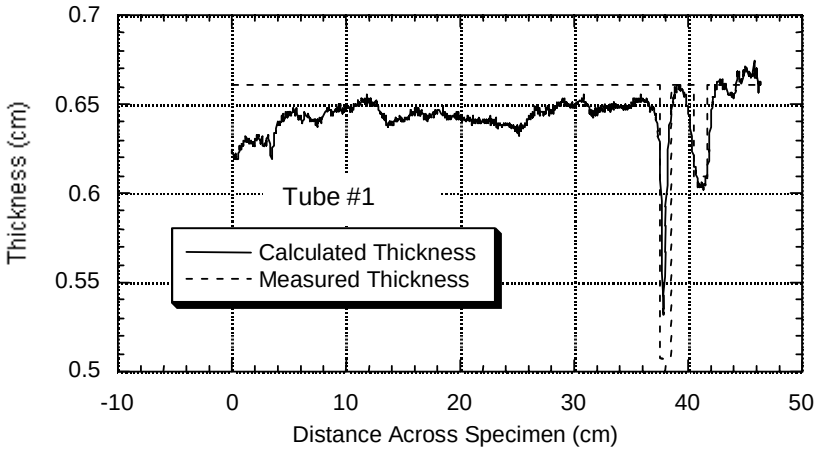

Figure 9 – Comparison of thickness measurements made both thermally and mechanically on boiler water-wall tubing specimen #2 for tube numbers 1 and 3 respectively.

Next, this technique was applied *in situ* to a power plant boiler. A carriage was constructed to translate the infrared camera and line heater vertically over the surface of the boiler water-wall tubing at a rate of 2.54 cm/s. The water-wall tubing was prepared by using high-pressure water to remove any loose material and then a light coat of water-soluble black paint was applied. Figure 10 shows the results of comparing thickness measurements made using this technique with conventional ultrasonic measurements for three of the tubes inspected. Calibration of the thermal data was performed in the same manner as described above, using two calibration standards with known thicknesses. Time constraints limited boiler access thus restricting the inspection area to a region of approximately 6 m^2 near the bottom of the boiler. The water-wall tubes in the boiler were 7.62 cm in diameter and were free standing (no webbing connecting one tube to the next). Limited ultrasonic thickness measurements were subsequently made in the same inspection area. While not exact, the agreement between the two measurement methods provides promising results. This has led to pursuing the thermal technique for large-scale application in boilers.

One reason for the disparity between the ultrasonic and thermal measurements could be the large number of "sprung tubes" in the inspection area. "Sprung tubes" occur in nonwebbed boilers due to the thermal expansion of the tubes during boiler operation. "Sprung tubes" are tubes that are no longer parallel to their next neighbor and can bend as much as 5 cm relative to the normal plane of the boiler wall. When the inspection apparatus moves over these "sprung tubes" the heat source to inspection surface distance changes, which can affect the accuracy of the thickness measurement made.

To address this problem a mechanical scanning mechanism was developed which allows the carriage to move independent of the water-wall. The scanner is 7.3 m in length, 1.4 m in width, weighs 650 pounds fully assembled, and can be disassembled to allow ingress through a boiler opening which is approximately 50 cm x 50 cm. An image of the full-scale scanner assembled inside a boiler is shown in Figure 11. This apparatus has been field tested in several operational power plants.

During a recent evaluation of the system at the Electric Power Research Institute (EPRI) Nondestructive Evaluation Center a water-wall specimen (specimen #3) was examined to determine the accuracy of the thickness measurements[7]. The specimen was 139.7 cm in length and 26.7 cm in width with tubes of outside diameter 3.2 cm and a nominal wall thickness of 0.64 cm. A matrix of defects of different lengths, widths and depths were machined into the specimen as shown in Table 1. Figure 12 shows a comparison of the results obtained using the line scanner to measure the thickness of the specimen and mechanical measurements made using a micrometer for some of the defects.

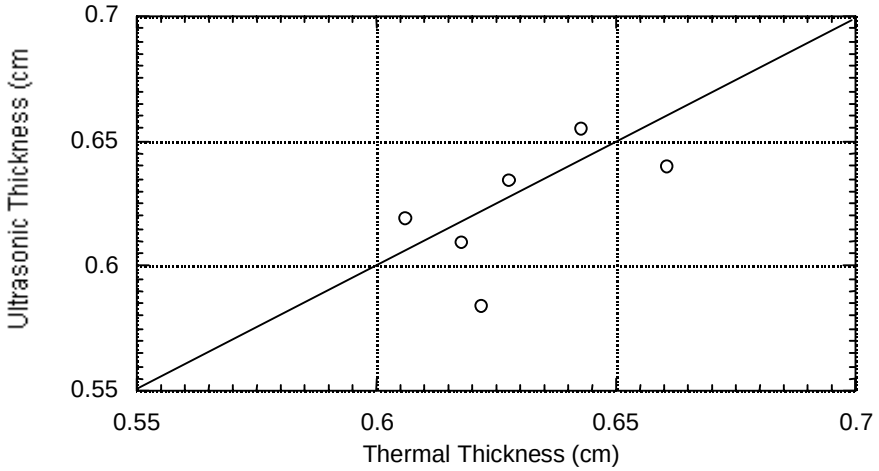

Figure 10 – Comparison of thermal and ultrasonic thickness measurements during *in situ* boiler inspection.

Figure 11 – Image of full scale scanning during an inspection inside a boiler

Table 1 -- Defect matrix for thickness accuracy measurements for specimen #3. Values shown are width of defect, length of defect and amount of material removed (units are cm) assuming a nominal thickness of 0.64 cm. Actual remaining thickness varied due to the variations in original tube thickness and machining proceedures.

Tube 1	Tube 2	Tube 3	Tube 4	Tube 5	Tube 6
1.59 x 2.86 x 0.38	1.27 x 4.45 x 0.38	0.95 x 4.76 x 0.38	0.95 x 2.22 x 0.38	0.64 x 3.81 x 0.38	0.64 x 0.64 x 0.19
1.59 x 3.49 x 0.38	1.59 x 1.59 x 0.19	1.27 x 1.27 x 0.19	0.95 x 3.18 x 0.38	0.64 x 4.45 x 0.38	0.64 x 1.27 x 0.19
1.59 x 4.13 x 0.38	1.59 x 2.22 x 0.19	1.27 x 1.91 x 0.19	0.95 x 3.49 x 0.38	0.64 x 5.08 x 0.38	0.64 x 1.91 x 0.19
1.90 x 1.91 x 0.19	1.59 x 2.86 x 0.19	1.27 x 2.54 x 0.19	0.95 x 4.13 x 0.38	0.95 x 0.95 x 0.19	0.64 x 2.54 x 0.19
1.90 x 2.54 x 0.19	1.59 x 3.49 x 0.19	1.27 x 3.18 x 0.19		0.95 x 1.59 x 0.19	0.64 x 3.18 x 0.19
1.90 x 3.18 x 0.19	1.59 x 4.13 x 0.19	1.27 x 3.81 x 0.19		0.95 x 2.22 x 0.19	0.64 x 3.81 x 0.19
1.90 x 3.81 x 0.19	1.59 x 1.59 x 0.38	1.27 x 4.45 x 0.19		0.95 x 2.86 x 0.19	0.64 x 4.45 x 0.19
1.90 x 1.91 x 0.38	1.59 x 2.22 x 0.38	1.27 x 1.27 x 0.38		0.95 x 3.49 x 0.19	0.64 x 5.08 x 0.19
1.90 x 2.54 x 0.38		1.27 x 1.91 x 0.38		0.95 x 4.13 x 0.19	0.64 x 0.64 x 0.38
1.90 x 3.18 x 0.38		1.27 x 2.54 x 0.38		0.95 x 4.76 x 0.19	0.64 x 1.27 x 0.38
1.90 x 3.81 x 0.38		1.27 x 3.18 x 0.38		0.95 x 0.95 x 0.38	0.64 x 1.91 x 0.38
		1.27 x 3.81 x 0.38		0.95 x 1.59 x 0.38	0.64 x 2.54 x 0.38
					0.64 x 3.18 x 0.38

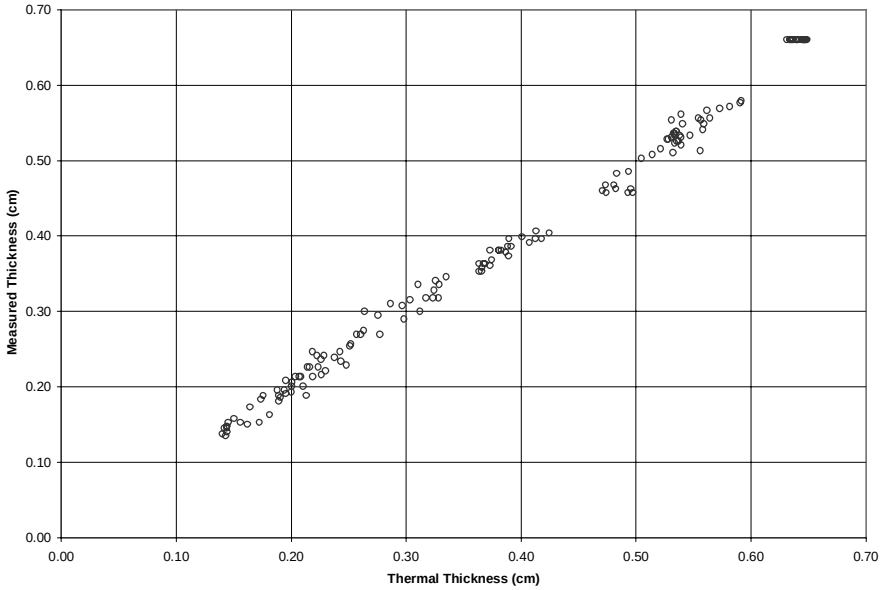

Figure 12 – Comparison of thermally and mechanically measured thickness from water-wall specimen #3 using full scale scanning system.

6. CONCLUSIONS

A noncontacting thermal NDE technique has been developed which employs a moving line heat source and is capable of imaging defects in boiler water-wall tubing. This technique has been shown to effectively detect thinning in steel laboratory samples designed to determine the resolution of the system. A steady state solution for the induced thermal change in a plate has been developed. When the steady state condition is achieved, the induced temperature change is inversely proportional to the thickness of the material at an observation point more than one thickness of the plate behind the line heat source. The experimental results are in good agreement with theoretical results.

Application of the technique to laboratory samples of water-wall tubing showed good agreement with both conventional ultrasonic thickness measurements and with mechanical measurements. Tests have shown that while sand blasting the surface of the tubing provides the optimal results, acceptable results can still be

obtained with high-pressure water washing. An initial test of this technique in an actual boiler has yielded promising results and has prompted the development of a field-ready boiler inspection apparatus based on this technique. This apparatus performs well on both welded and free standing water-wall tubes and has been shown to increase the accuracy of the thickness measurements.

7. ACKNOWLEDGMENTS

The authors would like to thank Carl D. Skelonis of Pennsylvania Power and Light Company and Gary Sharp at Virginia Electric Power Company for their help in obtaining access to operational power plant boilers for inspection and testing purposes.

Additionally, the authors would like to thank Paul Zayicek of the EPRI NDE Center for his support in evaluating the capabilities of the full-scale scanning system.

8. REFERENCES

1. L.D. Favro, T. Ahmed, X. Han, L. Wang, X. Wang, P.K. Kuo and R.L. Thomas, *Review of Progress in QNDE*, Vol. 15, eds. D.O. Thompson and D.E. Chimenti (Plenum, New York, 1996), p. 1747.
2. N. K. Del Grande, P.F. Durbin and D.E. Perkins, *Review of Progress in QNDE*, Vol. 12, eds. D.O. Thompson and D.E. Chimenti (Plenum, New York, 1993), p. 465.
3. K.E. Cramer, P.A. Howell and H.I. Syed, *Proceedings SPIE - Thermosense XVII*,Vol. 2473, , ed. S. A. Semanovich (SPIE,Bellingham,1995), p. 226.
4. X.P.V. Maldague, *Nondestructive Evaluation Of Materials By Infrared Thermography*, (Springer-Verlag, London, 1993).
5. K.E. Cramer and W.P. Winfree, *Proceedings SPIE - Thermosense XX* ,Vol. 3361, , eds. J.R. Snell, Jr. and R.N. Wurzbach (SPIE,Bellingham,1998), p. 291.
6. M.J. Nugent and S. Hansen, *Proceedings of 4th Conference on Fossil Plant Inspection*, (EPRI, Palo Alto, 1994).
7. P.I.Zayicek, *Evaluation of an Advanced Infrared Thermography System for Inspection of Boiler Tubes:* EPRI NDE Center, Charlotte, NC: 2000. {1000614}.